Multiwavelength visible laser based on the stimulated Raman scattering effect and beta barium borate angle tuning

Xiaoli Li (李小丽)*

Institute of Laser Engineering, Beijing University of Technology, Beijing 100124, China
**Corresponding author: lilyli@bjut.edu.cn*

Received October 22, 2015; accepted November 26, 2015; posted online February 1, 2016

We demonstrate wavelength-selectable visible emissions from a miniature crystalline laser that combines the stimulated Raman scattering (SRS) effect in an Nd:YVO_4 crystal with intracavity frequency mixing in an angle-tuned beta barium borate (BBO) crystal. The presented laser is operating on demand at any one of three wavelengths in the green-yellow spectral region. Up to 600, 560, and 200 mW output powers at 559, 532, and 588 nm, respectively, are obtained from the continuous wave (CW) laser having a 18 mm long resonator and a 3.8 W laser diode end pumping. The pump threshold for each visible wavelength is less than 0.4 W.

OCIS codes: 140.3550, 190.2620, 140.3380.
doi: 10.3788/COL201614.021404.

Stimulated Raman Scattering (SRS) in crystalline materials has been one of the most promising methods for nonlinear frequency conversion. It has been widely applied to generate new wavelengths that are not easily accessed in conventional lasers, such as 1.1–1.2 μm infrared, 1.5 μm eye-safe wavelengths, and 2–3 μm mid-infrared wavelengths[1–4].

For a high-Q Raman cavity incorporating laser and Raman crystals, the fundamental, first-Stokes, and even higher-order Stokes wavelengths can resonate simultaneously. Combining with intracavity frequency-mixing conversion through a nonlinear crystal, for which phase-matching conditions can be set for either second harmonic generation (SHG) or sum frequency generation (SFG) of the various circulating fields, it can enable the wavelength-selectable visible emissions from a single laser. This concept was demonstrated for the first time to our knowledge by Amman[5] in a pulsed laser, where five discretely tunable wavelengths were obtained with average output powers limited to 100 mW. In 2005, Mildren *et al.*[6] combined the processes of SRS and SFG to demonstrate a wavelength-selectable pulsed laser with average output power up to 1.8 W. Most recently, the first continuous wave (CW) wavelength-versatile laser was demonstrated by Lee using the Nd:$GdVO_4$ self-Raman geometry in connection with lithium triborate (LBO) temperature tuning[7]. Nevertheless, for the reported wavelength-versatile laser sources, the high threshold, large volume, and high pump power requirements are key factors constraining their practical applications.

In this Letter, we are focusing on the efficient power-downscaling of these devices in the CW regime, motivated by a number of applications in Raman spectrometer and laser-based multitasking machines. However, there are significant challenges arising from achieving acceptable thresholds and overall diode-visible optical conversion efficiencies for simultaneous SRS and SFG/SHG at low pump powers (a few watts), especially in the CW regime.

To overcome the challenge, we used an Nd:YVO_4 crystal as both a laser gain and Raman gain medium that can reduce the number of surfaces and round-trip losses within the cavity. Moreover, the method of beta barium borate (BBO) angle tuning was applied for intracavity SHG and SFG to generate wavelength-selectable output in the visible. It features a simplified laser configuration and rapid wavelength switching between the discrete lines compared to the LBO temperature tuning. These lead to efficient wavelength-selectable operation at 588, 559, and 532 nm from a single crystalline CW laser with low thresholds (<0.4 W), compact cavity (~18 mm), and comparable conversion efficiency.

The layout of the miniature wavelength-selectable Raman laser is schematically illustrated in Fig. 1. The pump source used in this work was an 808 nm, high-brightness free-space diode laser (UniqueMode, UM4200-M20-CB-TEC) that produced horizontally polarized pump light with a maximum output power of 3.8 W. The diode output was collimated through a telescope arrangement, and then focused into an Nd:YVO_4 crystal through a 50 mm focal length lens.

The 4 mm × 4 mm × 3 mm (long), a-cut, 1 at.% doped Nd:YVO_4 crystal played the role of both laser crystal and Raman crystal. Its high Raman gain (4.5 cm/GW[8]) at 890 cm^{-1} Raman shift and high-emission cross section (14.1×10^{-19} cm^2[9]) at 1064 nm wavelength can provide a low threshold and high fundamental intracavity power under modest pump power. The pump facet of the Nd:YVO_4 was directly coated for high reflectivity (HR) at both fundamental and first-Stokes wavelengths, which led to the replacement of a separate input mirror used in

conventional laser cavities. The other surface of the Nd:YVO_4 crystal was antireflection (AR) coated ($R = 0.026\%$ at 1064 nm, $R = 0.045\%$ at 1176 nm) to reduce the cavity losses for both wavelengths. According to Ref. [9], an Nd:YVO_4 crystal has an approximately four times larger absorption coefficient for 808 nm pump light polarized along the crystal c axis rather than that of the a axis. Therefore, we oriented the pump light linearly polarized along the crystal c axis for the higher pump absorption. For heat removal, the Nd:YVO_4 crystal was wrapped by indium foil and housed in a water-cooled copper heat sink maintained at 20°C.

A 4 mm × 4 mm × 5 mm (long) BBO crystal was employed for intracavity SHG/SFG to generate visible emissions. The BBO crystal was AR coated for 1064, 1176, and 530–590 nm, and it was initially cut for type I phase matching ($\theta = 21.5°, \varphi = 0°$) for SHG of 1176 nm. Owing to its relatively large effective nonlinear coefficient of 2.20 pm/V[10], compared to 0.85 pm/V of LBO[11], high conversion efficiency from the infrared to the visible is achievable with a short crystal. A BBO crystal also features a small acceptance angle that enables wavelength selection in a single resonator by slightly tuning the crystal angle for different phase-matching requirements. According to the select nonlinear optics (SNLO) software calculation outlined in Fig. 1, the optimum angle for type I phase matching in a BBO crystal differs slightly for the different visible outputs of interest. From the 588 nm yellow to the 559 nm lime generation, the angle difference is only 0.6°. A further change of 0.9° is required for the 532 nm green generation. All of these conditions can be easily matched in our miniature CW Raman lasers by manually angle tuning the BBO crystal, and only minimal realignment of the cavity was required. In addition, the BBO crystal has a relatively large temperature range, which means that the strength of SHG/SFG within this crystal is not temperature-sensitive and temperature control is not required in our system. Compared to the mean of the LBO temperature and angle tuning employed in Refs. [6,7,12], the BBO angle-tuning brought us a simple and compact system design with rapid switching between selectable wavelengths.

The laser resonator in our experiments had a linear and compact configuration, as shown in Fig. 1. We investigated the laser performance at fundamental wavelengths using a high-Q cavity formed by the HR-coated facet of the Nd:YVO_4 and a curved mirror M1, while different curved mirrors M2 and M3 were used as output couplers for Stokes and visible emissions, respectively. The details of all of the cavity mirrors and coatings are summarized in Table 1. In addition to the use of short crystals, all of the components within the cavity were positioned as close to one another as possible to minimize the cavity length. The total cavity length, including the BBO crystal, was merely 18 mm, giving the benefits of small cavity mode sizes, high power densities, and increased laser stability that were essential to realize low threshold and high conversion efficiency for our miniature CW laser.

We used thin-film optical filters to separate the different output wavelengths and then measured the corresponding output powers with a silicon power meter. The spectral properties of the output were measured using Ocean Optics fiber-coupled spectrometers (USB2000) and the beam quality was measured using a scanning slit-beam profiler (Gentec Beamscope P8).

As shown in Fig. 2, we achieved the fundamental emission at 1064 nm from the resonator using output coupler M1, for which the pump-power threshold was observed to be 0.2 W. As the pump power increased to 3.8 W, we obtained 2.2 W output at 1064 nm with a diode to optical

Table 1. Summary of Cavity Mirrors and Coatings

Mirror	Details
HR coating	$T = 99.539\%$ at 808 nm, $R > 99.994\%$ at 1064 nm, $R > 99.9994\%$ at 1176 nm
M1	300 mm radius of curvature (ROC) mirror: $T = 5\%$ at 1064 nm
M2	250 mm ROC mirror: $R = 99.91\%$ at 1064 nm, $R = 99.6\%$ at 1176 nm.
M3	50 mm ROC mirror: $R > 99.994\%$ at 1064 and 1176 nm, $T > 95\%$ at 532, 559, and 588 nm.

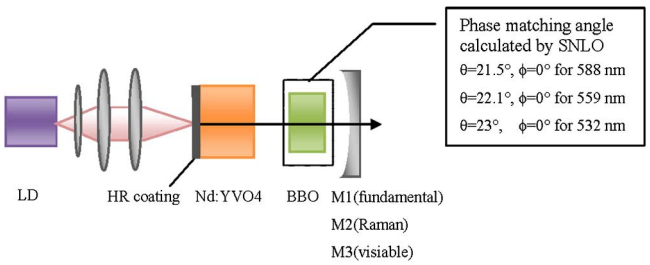

Fig. 1. Schematic diagram of a wavelength-selectable miniature Raman laser using $NdYVO_4$ self-Raman crystal and angle-tuned BBO crystal.

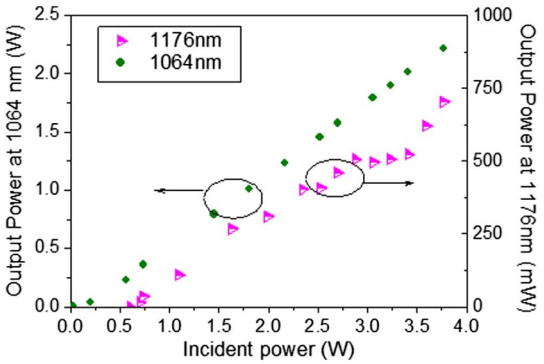

Fig. 2. Fundamental (circles) and Stokes (triangles) output powers as functions of incident pump power, from the laser cavities without a BBO crystal.

conversion efficiency of 57.9%. The Raman cavity was formed by the incident facet of the laser crystal and output coupler M2, providing high-Q for both fundamental and first-Stokes optical fields. Figure 2 shows that the threshold for Raman lasing was reached at 0.6 W and up to 700 mW Stokes output was obtained with 3.8 W pump power, responding to a diode-to-Stokes conversion efficiency of 18.4%.

In comparison with our previous results based on a conventional setup using a discrete input mirror[13], this work revealed lower thresholds and a higher optical conversion efficiency for both the fundamental and first-Stokes emission under the same setup of pump geometry. We attribute such improvement to several factors, including higher transmission for the 808 nm pump light through an HR-coated facet of crystal rather than a discrete input mirror ($T = 99.539\%$ vs $T = 98\%$), fewer intracavity surfaces, and lower resonator losses.

For wavelength-selectable operation in the visible, the BBO crystal was inserted into the cavity formed by the HR-coating and M3. The angle of the BBO crystal was tuned to separately optimize the phase-matching condition for SHG of 1064/1176 nm and SFG of both. Figure 3 shows the laser power scaling performance at green (532 nm), lime (559 nm), and yellow (588 nm) wavelengths. The threshold of lasing at any one of the three wavelengths was less than 0.4 W, responding to a factor of 5 lower than the threshold of the wavelength-versatile visible laser using a long and weekly-doped laser crystal combined with a temperature-tuned LBO in Ref. [7]. At 3.8 W pump power, up to 600 and 560 mW output power were achieved for the lime and green emissions, respectively, while the maximum yellow output power was 200 mW. The corresponding diode-to-visible conversion efficiencies were 15.8%, 14.7%, and 5.3%, respectively. Note that the 532 nm output power was slightly lower than that of 559 nm, especially when the pump power was more than 3 W. This can be attributed to that the coating transmittance at 559 nm of cavity mirror M3 is slightly larger than that at 532 nm, according to the coating parameters provided by Advanced Thin Films Corp. Also note that the collected output powers were only for the visible light propagating toward the output coupler. If an intracavity mirror is used to reflect the backward visible generation, more output power and a higher conversion efficiency can be expected.

The beam quality and spectral properties of all three visible generations were also measured in the experiments. As shown in Fig. 4, the linewidths of the three visible were all around 0.2–0.3 nm. The beam quality parameter (M^2) of the visible outputs were 1.5, 2.0, and 4.3 at 588, 532, and 559 nm, respectively, measured at maximum incident pump power. The yellow output had the best beam quality, while the M^2 for the lime output was found to be relatively higher, which was also observed in Ref. [14]. Most likely this can be attributed to the Raman beam cleanup effect bringing more benefit to the SHG beam quality rather than the SFG. We also observed the beam profile at the beam waist; it was apparent that the lime output had high-order transverse modes. This may be also related to the relatively large walk-off angle of the BBO crystal.

To conclude, all solid state multiwavelength lasers have experienced a blooming development in recent years, motivated by the breakthrough of new crystal growth and nonlinear optics technologies[15–17]. In this Letter, we demonstrate a miniature, efficient, crystalline Raman laser operating at three discretely tunable wavelengths in the green-yellow spectral region, on the basis of Raman frequency conversion combined with intracavity SHG/SFG. The experimental results show that at 3.8 W pump power, the maximum visible output powers at

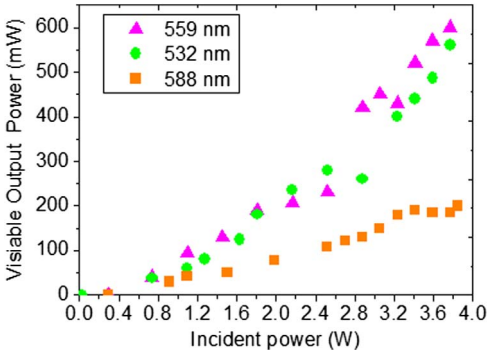

Fig. 3. Visible output powers of the miniature wavelength-selectable laser as functions of incident pump power.

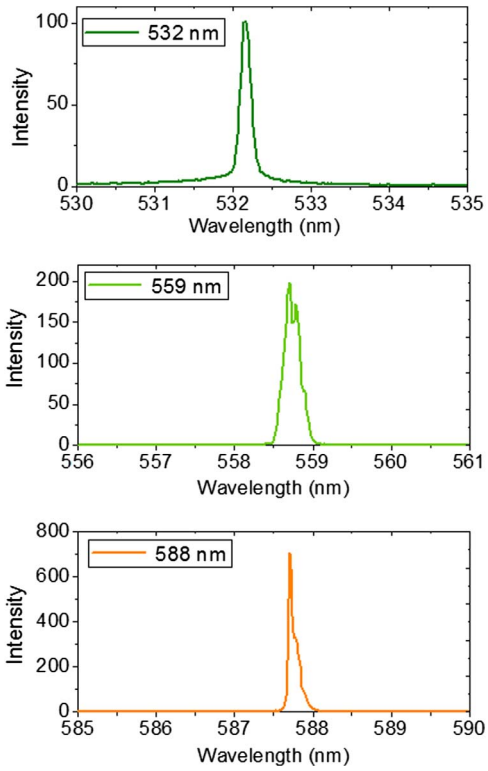

Fig. 4. Measured spectral characteristics of visible emissions at green (top), lime (middle), and yellow (bottom) wavelength.

559, 532, and 588 nm are reached at 600, 560, and 200 mW, responding to the diode-to-visible conversion efficiencies of 15.8%, 14.7%, and 5.3%, respectively. The wavelength switching between the three lines can be easily realized in the same resonator by BBO angle tuning for different phase-matching requirements. The thresholds of all of the visible emissions are less than 0.4 W.

These results pave the way for the realization of a wavelength-versatile visible source with a compact configuration, low threshold, and competitive conversion efficiency for practical use. Such miniature wavelength-selectable laser can serve as an ideal light source of laser-based machines and optical systems, such as Raman spectrometers, measurement instruments for material refractive index, and laser processing devices, with the ability to expand their working spectral range and realize multifunction and complex tasks only using one laser. It can be anticipated that with mirrors coated for high-order Stokes resonating simultaneously at increased pump power, more expanded visible spectra can be achieved from a miniature crystalline Raman laser. More output power and improved conversion efficiency can also be expected if an intracavity mirror is used to assist the backward-visible output collection.

References

1. H. Shen, Q. Wang, P. Li, G. Lv, X. Zhang, Z. Liu, X. Chen, Z. Cong, L. Gao, X. Tao, H. Zhang, and J. Fang, Opt. Commun. **306**, 165 (2013).
2. O. Kitzler, H. Jelinkova, J. Sulc, L. Koubikova, M. Nemec, K. Nejezchleb, and V. Skoda, Proc. SPIE **8599**, 85991W (2013).
3. J. Zhao, X. Zhang, X. Guo, X. Bao, L. Li, and J. Cui, Opt. Lett. **38**, 1206 (2013).
4. A. Sabella, J. A. Piper, and R. P. Mildren, Proc. SPIE **8959**, 89590B (2014).
5. E. O. Ammann, J. Appl. Phys. **51**, 118 (1980).
6. R. P. Mildren, H. M. Pask, H. Ogilvy, and J. A. Piper, Opt. Lett. **30**, 1500 (2005).
7. A. J. Lee, D. J. Spence, J. A. Piper, and H. M. Pask, Opt. Express **18**, 20013 (2010).
8. A. A. Kaminskii, K.-i. Ueda, H. J. Eichler, Y. Kuwano, H. Kouta, S. N. Bagaev, T. H. Chyba, J. C. Barnes, G. M. A. Gad, T. Murai, and J. Lu, Opt. Commun. **194**, 201 (2001).
9. Y. Sato and T. Taira, IEEE J. Sel. Top. Quantum Electron. **11**, 613 (2005).
10. R. C. Eckardt, H. Masuda, Y. X. Fan, and R. L. Byer, IEEE J. Quantum Electron. **26**, 922 (1990).
11. D. A. Roberts, IEEE J. Quantum Electron. **28**, 2057 (1992).
12. H. M. Pask, P. Dekker, R. P. Mildren, D. J. Spence, and J. A. Piper, Prog. Quantum Electron. **32**, 121 (2008).
13. X. Li, A. J. Lee, H. M. Pask, J. A. Piper, and Y. Huo, Opt. Lett. **36**, 1428 (2011).
14. A. J. Lee, H. M. Pask, D. J. Spence, and J. A. Piper, Opt. Lett. **35**, 682 (2010).
15. Y. Zhao, Z. Wang, H. Yu, X. Xu, J. Xu, and X. Xu, Chin. Opt. Lett. **13**, 021404 (2015).
16. F. Zhang, Q. Zhang, B. Wang, D. Hu, H. Yu, H. Zhang, Z. Wang, and X. Xu, Chin. Opt. Lett. **12**, 121902 (2014).
17. P. Zhang, W. Ma, T. Wang, Q. Jia, and C. Wan, Chin. Opt. Lett. **12**, 111403 (2014).